The spatial distribution of coupling between tau and neurodegeneration in amyloid-β positive mild cognitive impairment

Belfin Robinson[1], Shankar Bhamidi[2], and Eran Dayan[1,3], for the Alzheimer's Disease Neuroimaging Initiative

[1]Biomedical Research Imaging Center, University of North Carolina at Chapel Hill, Chapel Hill, North Carolina 27514, USA.
[2]Department of Statistics and Operations Research, University of North Carolina at Chapel Hill, Chapel Hill, North Carolina 27599-3260, USA
[3]Department of Radiology, University of North Carolina at Chapel Hill, Chapel Hill, North Carolina 27599, USA.

Corresponding author
Eran Dayan,
Associate Professor of Radiology,
University of North Carolina at Chapel Hill.
Email: eran_dayan@med.unc.edu

Short/running title.
Coupling between tau and neurodegeneration in MCI

Keywords: tau, atrophy, Alzheimer's disease, multilayer networks

ABSTRACT

Synergies between amyloid-β (Aβ), tau, and neurodegeneration persist along the Alzheimer's disease (AD) continuum. This study aimed to evaluate the extent of spatial coupling between tau and neurodegeneration (atrophy) and its relation to Aβ positivity in mild cognitive impairment (MCI). Data from 409 participants were included (95 cognitively normal controls, 158 Aβ positive (Aβ+) MCI, and 156 Aβ negative (Aβ-) MCI). Florbetapir PET, Flortaucipir PET, and structural MRI were used as biomarkers for Aβ, tau and atrophy, respectively. Individual correlation matrices for tau load and atrophy were used to layer a multilayer network, with separate layers for tau and atrophy. A measure of coupling between corresponding regions of interest (ROIs) in the tau and atrophy layers was computed, as a function of Aβ positivity. Fewer than 25% of the ROIs across the brain showed heightened coupling between tau and atrophy in Aβ+, relative to Aβ- MCI. Coupling strengths in the right rostral middle frontal and right paracentral gyri, in particular, mediated the association between Aβ burden and cognition in this sample.

INTRODUCTION

Alzheimer's disease (AD), the most common form of neurodegeneration, has become a key contemporary public health concern (Nichols et al., 2019. While the cause of this disease is still unknown, it is believed to develop from the accumulation of the extracellular amyloid-β (Aβ) peptide and from tangles of hyperphosphorylated tau, which lead to synaptic impairment, neuronal loss (atrophy), and consequently to cognitive and behavioral decline (Kumar et al., 2015). The leading model as to how these pathological processes bind together is known as the amyloid cascade hypothesis (Ricciarelli and Fedele, 2017). According to this influential framework, Aβ pathology initiates alterations in tau which then lead to neurodegeneration and to the cognitive and behavioral manifestations of AD (Karran et al., 2011).

The serial and linear structure of the amyloid cascade hypothesis has, nevertheless, been challenged in the literature. In particular, studies suggest that A□, tau, and neurodegeneration (atrophy) could have synergistic effects in AD pathogenesis (Busche and Hyman, 2020). Yet, the extent of spatial coupling between alterations in AD pathological biomarkers, specifically in biomarkers for tau and atrophy remains uncertain (LaPoint et al., 2017; Mak et al., 2018; Sepulcre et al., 2016; Xia et al., 2017). On the one hand, studies have reported large degrees of spatial overlap throughout the brain between tau burden, as assessed using positron emission tomography (PET), and magnetic resonance imaging (MRI)-based measures of atrophy in both cognitively normal controls and individuals with AD (Xia et al., 2017). On the other hand, studies have found more restricted spatial coupling between tau and atrophy, which may emerge from heterogeneity in patterns of tau spread (Mohanty et al., 2023). Moreover, the majority of studies that examined interactions between tau and atrophy were either in normal controls or in individuals with AD (Digma et al., 2019; Liu et al., 2021). The extent of coupling between these biomarkers in individuals with MCI and AD pathologic changes, who can be considered as being at the prodromal stages of AD(Jack et al., 2018), remains less understood.

Over the last decade, there has been significant interest and methodology development in the study of network valued data over the same node set (e.g., regions in the brain), but across multiple layers (De Domenico, 2017; Kivelä et al., 2014). These methods may help in clarifying the extent of coupling that exists between tau and atrophy, as they offer additional insight on complex relationships within and between variables in multiple layers, which may be missed by studies looking at single-layer covariance. Multilayer networks allow to model and study complex heterogeneous relationships between entities within a system and variation of these relationships across layers (Boccaletti et al., 2014; Kivelä et al., 2014). In the context of brain networks, multilayer network models were used for studying the relationships between brain structure, function, and dynamics across multiple scales, both in the healthy brain and in AD (Cai et al., 2020; De Domenico, 2017; Guillon et al., 2019). We reasoned that the extent of spatial coupling between tau and atrophy could be modeled using multilayer networks, since this approach can allow to inspect interactions both within and between network layers.

In the current study, we used a cross-sectional sample of participants with MCI (n=314), as well as data from cognitively normal (CN) participants (n=95) to reconstruct single-subject multilayer networks that represent tau and atrophy as separate layers, and the interactions among these two biomarkers in between layers. More specifically, tau PET and structural MRI (atrophy) data from 70 regions of interest (ROIs) were first extracted from MCI and CN participants. Tau and atrophy data were then z-score transformed relative to the means and standard deviations from the entire pool of CN participants. Subsequently, individual-subject covariance matrices were computed for each participant and used to reconstruct tau and atrophy networks for each participant after minimally thresholding the edge weights to retain all positive weights in the networks. The tau and atrophy networks were then modeled as multilayer networks and grouped according to Aβ positivity. This allowed us to study the interaction between the tau and atrophy layers at the presence and absence of Aβ positivity.

METHODS AND MATERIALS

-- Figure 1 Here --

Participants

Data used in this study were obtained from the Alzheimer's Disease Neuroimaging Initiative (ADNI) dataset (https://ida.loni.usc.edu), including the ADNI-1, ADNI-GO, and ADNI-2 cohorts. A total of 314 MCI participants who had ^{18}F-florbetapir and ^{18}F-flortaucipir PET data were included in the study **(Table 1)**. Data from 95 CN participants was additionally used to aid in the reconstruction of individual-subject graphs/networks for each of the MCI participants. ADNI's native inclusion and exclusion criteria were used in both the CN and MCI groups. Briefly, MCI participants had Mini-Mental State Examination (MMSE) scores ranging from 24 to 30, reported memory-related concerns, exhibited memory decline based on Wechsler Memory Scale Logical Memory II scores adjusted for education, had a Clinical Dementia Rating (CDR) score of 0.5, displayed no substantial impairment in other cognitive domains, maintained their ability to perform activities of daily living, and did not have dementia. CN participants had MMSE scores ranging from 24 to 30, CDR scores of 0, were free from depression, did not have MCI, and were not diagnosed with dementia.

Participants with MCI were further divided into Aβ positive (Aβ+) and negative (Aβ-), based on an established cutoff (Standardized uptake value ratio [SUVR]**> 1.11**), computed relative to an inferior cerebellum reference region (Landau et al., 2013b, 2012b). All CN participants were amyloid and tau negative. All participants provided written informed consent and the procedures were all approved by the local Intuitional Review Boards.

Imaging data analysis

Regional florbetapir PET summary data were obtained from ADNI as derived variables (Landau et al., 2013a, 2012a). In short, T1 weighted native-space images were processed with FreeSurfer v7.1.1, and a cortical summary region was defined for each subject, based on frontal, anterior and posterior cingulate, lateral parietal, and lateral temporal ROIs. The T1 images were coregistred to florbetapir PET scans, which allowed to extract PET data from cortical ROI. SUVR's were then calculated for the cortical summary region, based on an inferior cerebellum reference region. SUVR values from the cortical summary region were then used to define Aβ burden and positivity. Regional summary data based on flortaucipir PET were also obtained from ADNI as derived variables. In short, MPRAGE images were parcellated into a set of 70 ROIs using FreeSurfer v7.1.1 based on the Desikan-Killiany protocol (Desikan et al., 2006). The right and left hippocampi were removed from the analyses, since tau load data in these regions may be contaminated by off-target binding (e.g. Biel et al., 2022; de Flores et al., 2022). Flortaucipir images were co-registered to the corresponding MPRAGE images to determine the mean regional flortaucipir uptake within each ROI. SUVRs for each of the 70 ROIs were then calculated, by dividing uptake values by an inferior cerebellar reference region. Finally, grey matter volumes extracted from the same 70 ROIs using FreeSurfer v7.1.1 were used as measures of regional atrophy.

Network reconstruction

Regional tau uptake and grey matter volume data from MCI participants were considered for analysis (**Figure 1A**). Data from CN participants were further used to aid in the reconstruction of single-subject networks/graphs for each subject with MCI (**Figure 1A**). In this procedure, individual covariance networks in the target group, are reconstructed based on their deviation from an averaged network based on a group of controls (Yun et al., 2020). First, an averaged covariance network was reconstructed from a group of CN participants (n=95), separately for tau and atrophy. Atrophy and tau data from each MCI subject were then normalized via a z-score transformation using the mean and standard deviation of the CN-based, tau and atrophy networks (**Figure 1B**). This allowed for the reconstruction of single covariance matrices (Yun et al., 2020, 2015) for each MCI subject (**Figure 1C**). The covariance matrix is a nROI × nROI matrix, where for each index [x,y] we compare the z-scores of the corresponding tau and atrophy ROIs. The equation is given below:

$$Brain\ structural\ covariance[x, y] \ = \frac{1}{e^{[(zscore\ of\ x^{th}\ ROI - zscore\ of\ y^{th}\ ROI)^2]}} \qquad (1)$$

Higher values in ROIs within these matrices denote high covariance compared to the corresponding ROIs from the averaged CN-based networks. The matrices generated for tau and atrophy were structured as single-layer networks/graphs **(Figure 1D).** The single-layer graphs were then layered into a two-layered graph with tau and atrophy as separate layers **(Figure 1E).** This form of representation allowed us to examine and compare both intra-layer (green colored edges in **Figure 1F**), and inter-layer edges (yellow-colored edges in **Figure 1F**). While the former type of edges corresponds to covariance for ROIs in the tau and atrophy networks separately, the latter type of edges, which connect the nodes across layers, allow to examine interactions between tau and atrophy. Moreover, unlike multiplex networks, where inter-layer edges connect the same nodes across layers, the multilayer network representation used here also incorporates inter-layer edges connecting across nodes (grey dotted edges in **Figure 1F**). The multilayer networks were generated using R (Version 4.2.1) (Team, 2021), with the igraph (Version: 1.3.5) and muxviz (Version: 3.1) (De Domenico et al., 2015) libraries.

Interlayer coupling score.

A key objective in the current study was to assess the extent of regional/spatial coupling between tau and atrophy in the presence and absence of A□ positivity. To that effect we have computed a coupling score between the tau and atrophy layers, based on the distance between the layers (Shimada et al., 2016). As a measure of distance, we used Euclidean distance, as it was previously used to assess coupling between network node sets (Liu et al., 2022). First, the partitioned distance between the tau and atrophy layers was calculated. The resulting distance matrix D was used to calculate the coupling score. The distance between identical ROIs across layers was defined as (D_r), whereas interlayer edges, connecting different ROIs across the layers were defined as (D_b). The coupling score was computed to measure the relative coupling between tau and atrophy, as the ratio between a spatially coupled edge and all other non-coupled edges:

$$\text{Coupling score} = \frac{D_r - mean(D_b)}{D_r} \qquad (2)$$

Partitioned Euclidian distance was computed using the pdist (Version 1.2.1) library (https://github.com/jeffwong/pdist) in R (Version 4.2.1). A toy example of the procedure for calculating coupling scores is illustrated in **supplementary Figure 1**.

Statistical Analysis

Group differences in demographic data (age, gender, education) were analyzed using t-tests or chi-squared tests. These analyses were conducted in R, with the packages dgof (v1.4) (https://CRAN.R-project.org/package=dgof). Group differences in tau load and in atrophy, as well as in regional coupling between tau and atrophy were based on a non-parametric, permutation-based analysis of variance, adjusted for age (see **Table 1**). The resulting p-values were False Discovery Rate (FDR) corrected across ROIs. These tests were carried out using the aovperm function, which is part of the permuco (v1.1.1) library (https://github.com/jaromilfrossard/permuco) in R. Finally, we examined whether the association between Aβ burden and cognition, assessed with clinical dementia rating sum of boxes (CDR-SB) scores (O'Bryant, 2008), was mediated by the extent of coupling between tau and atrophy. Similar mediation analyses were carried out wherein regional tau and atrophy scores replaced coupling scores. Parallel mediation analyses were conducted in Python 3, using the pingouin package (Version 0.5.3) (https://pingouin-stats.org/). Confidence intervals in the mediation model were computed using bootstrapping (10,000 steps).

RESULTS

Group demographics

Our objective was to compare the extent of coupling between tau and atrophy in the presence and absence of Aβ positivity. To that effect, we divided a total of 314 individuals with MCI into two groups, Aβ + (n=158) and Aβ - (n=156), based on Aβ PET data and established cutoffs (Landau et al., 2013b, 2012b), see Methods and Materials). The Aβ + and Aβ - groups did not show significant differences in sex (p=0.364) or education (p=0.536) but did differ in age (p= 0.0288) and CDR-SB scores (p= 4.303e-08) **(Table 1)**.

Table 1 Characteristics of data used in the study.

Measure	**Aβ +**	**Aβ -**	**CN**
Age (years) *	71.13 ± 6.96*	70.28 ± 6.71*	70.45 ± 5.75
Sex	Female: 81 (51) Male: 77 (49)	Female:72 (46) Male: 84 (54)	Female:51 (54) Male: 44 (46)
Education (years)	16.34 ± 2.60	16.52 ± 2.65	16.84 ± 2.56
CDR-SB	2.99±3.84*	0.997±2.19*	0.268±1.01

Values are given as mean ± standard deviation or percentages (%); * denotes significant group difference (p<0.05); Aβ- amyloid-β

Tau load and atrophy levels in Aβ + and Aβ - participants

We first examined group difference between Aβ + and Aβ - participants in tau load and in atrophy. Mean levels of tau load **(Figure 2A)** were significantly higher in Aβ + relative to Aβ - participants, when adjusting for age t (191.2) = -7.6655, ($p<0.001$). Similarly, mean levels of atrophy **(Figure 2B)** were significantly higher (i.e., regional volumes were lower) in Aβ + relative to Aβ - participants, when adjusting for age t (308.75) = 3.1251, ($p=0.009$). In both comparisons, significant differences were retained when outlier values were removed.

Coupling between tau and atrophy

We next examined the regional coupling between tau and atrophy, and the extent to which it differed as a function of Aβ positivity. Taking advantage of the multilayer representation of tau and atrophy as separate layers composed of identical nodes (ROIs), we computed a coupling score between tau and atrophy, based on the Euclidean distance between the layers **(Figure 2C).** The coupling score denoted the ratio between each spatially coupled edge and all other non-coupled edges in the multilayer network (**Supplementary Figure 1**; see Methods and Materials). The Aβ+ group showed significantly greater coupling compared to the Aβ- group (FDR corrected) **(Figure 2D,** with coupling scores in each group separately shown in **Supplementary Figure 2)** in lateral and superior temporal, insular, parietal and frontal ROIs, predominately lateralized to the right (Supplementary Table 1). Altogether, only 24.2% of the ROIs showed stronger coupling between tau and atrophy in the Aβ+ group, relative to the Aβ- group**.**

-- Figure 2 Here --

Mediational link between Aβ burden cognition and tau-atrophy coupling

Our results so far reveal differential levels of coupling between tau and atrophy when comparing Aβ+ and Aβ- participants. Next, we examined whether the extent of coupling and its relationship with Aβ burden also relates to participants' cognitive status. First, the association between coupling (considering ROIs where coupling scores were found to be significant) and CDR-SB scores, used here as a measure of cognitive status, was significant in both Aβ + ($\beta=0.165$, $p=0.039$), and Aβ - ($\beta=0.199$, $p=0.013$) participants (**Supplementary Figure 3**). Next, considering Aβ as a continuous variable, we tested whether the association between Aβ burden and global cognition, assessed with CDR-SB scores corrected for age, were mediated by the extent of coupling between tau and atrophy. This was achieved by fitting the data with a parallel mediation model. We found that coupling in the right rostral middle frontal ($p = 0.005$) and right paracentral ($p = 0.0288$) ROIs significantly mediated the association between Aβ burden and CDR-SB scores **(Figure 3).** Similar models wherein regional tau and atrophy (tested separately) were included in the model as potential mediators, instead of coupling scores, did not yield any significant indirect effects.

-- Figure 3 Here --

DISCUSSION

The objective of the current study was to estimate the extent of spatial coupling between tau and atrophy biomarkers in individuals with MCI, study the role of Aβ burden in this coupling, and examine the relationship between coupling and cognitive dysfunction. Overall, stronger coupling between tau and atrophy was observed in Aβ+ as compared to Aβ- individuals with MCI. Differences in coupling between these two groups varied spatially and were observed in less than 25% of the ROIs considered for analysis. Finally, our results reveal that coupling between tau and atrophy in right rostral middle frontal and right paracentral gyri mediated the association between Aβ burden and cognitive dysfunction.

Our results show that fewer than 25% of the ROIs across the brain showed significant coupling between tau and atrophy, as a function of Aβ positivity. Previous research on the extent of coupling between tau and atrophy has yielded inconsistent results. Namely, substantial spatial overlap between PET-based tau burden and MRI-based atrophy measures has been reported in both cognitively normal controls and individuals with AD (Xia et al., 2017). Conversely, a smaller degree of spatial association between tau and atrophy was found in other studies (Mohanty et al., 2023). Our novel approach for assessing overlap between tau and atrophy suggests that the coupling among the two is more restricted than that observed when using other analytical techniques.

Asymmetry in tau burden (Lu et al., 2023) and in atrophy (Jahanshahi et al., 2023) is a consistent finding in studies in aging and dementia. Asymmetry in tau burden contributes significantly to accelerated memory decline, and to the heterogeneity observed in AD (Lu et al., 2023). Similarly, asymmetric atrophy, not restricted to the left or right hemisphere, was found in a large meta-analysis of studies of aging and multiple neurodegenerative diseases (Minkova et al., 2017). In the current study, we observed significant coupling between tau and atrophy, as a function of Aβ positivity, primarily in the right hemisphere. Associations have been reported between both tau (Ossenkoppele et al., 2019) and atrophy (Chang et al., 2018) covariance networks, and intrinsic functional connectivity in the brain. Our findings of right hemispheric dominance in coupling are thus in line with reports on abnormal rightward dominance in whole brain functional connectivity among MCI and AD participants (Liu et al., 2018). Whether the spatial extent of coupling between tau and atrophy also relates to patterns of connectivity in large-scale functional networks remains to be more specifically determined in future research.

When comparing Aβ+ and Aβ- participants with MCI significant coupling between tau and atrophy was observed in lateral and inferior temporal, insular, superior parietal and frontal ROIs. Consistent with these findings, associations between tau burden and cortical atrophy in AD and MCI were reported in inferior temporal, parietal, and frontal regions (Timmers et al., 2019). Atrophy in lateral temporal and to a lesser extent parietal and frontal regions was found to allow for the subtyping of participants with MCI into subgroups, showing distinct clinical phenotypes (Kwak et al., 2021). Regions such as the inferior and middle temporal cortices are also key regions of tau accumulation in MCI and AD (Maass et al., 2017). Increased tau burden in the inferior temporal lobe in AD is associated with greater impact on activities of daily living (Halawa et al., 2019), while tau burden in frontal cortex predicts longitudinal decline in executive function (Pereira et al., 2020). We should note that our choice to remove the hippocampus from the analysis, motivated by its off-target tau PET binding (See Methods and Materials), likely impacted our ability to detect coupling in additional regions impacted early in along the AD continuum. Thus, while the current results mostly highlight coupling in higher-order cortical regions, the extent of coupling in entorhinal and limbic regions should be further evaluated with suitable methods.

We report that the association between Aβ burden and global cognition, as captured by CDR-SB scores, is mediated by the extent of tau-atrophy coupling in right rostral middle frontal and right paracentral cortices. The rostral middle frontal gyrus shows heightened tau deposition in Aβ positive individuals (Young et al., 2021). Morphometric properties of this region were also reported to correlate with executive function performance in both MCI and healthy aged-matched controls (Chang et al., 2010). Similarly, right paracentral cortical atrophy is higher in individuals with MCI who progress to AD, relative to those who remain stable over time (Julkunen et al., 2009). This region also shows cortical thinning in AD, relative to controls (Yang et al., 2019). Altogether, our findings join these earlier observations in highlighting the contribution of pathology in the middle frontal and paracentral regions to cognitive dysfunction in MCI.

In the current study we queried the extent of coupling between tau and atrophy by modeling multimodal neuroimaging data as a multilayer network. Multilayer networks can aid in modeling complex interactions that occur among biological (or non-biological) processes that operate at differing spatial and temporal scales (Robitaille et al., 2021). This approach may thus properly capture the heterogeneity often observed in biological systems which may result from the diverse interactions of the system's various substrates (Hammoud and Kramer, 2020). Here, the multilayer representation allowed us to compare coupled versus non-coupled interactions among 2 distinct biological processes characteristic of the AD continuum. Future work can focus on other processes and mechanisms which can be quantified in multilayer networks, such as changes in modularity (Taylor et al., 2017; Wilson et al., 2017) redundancy (Radicchi and Bianconi, 2017), and robustness (Kumar and Singh, 2020; Liu et al., 2020), known to be strongly impacted by aging and dementia (Contreras et al., 2019; Langella et al., 2021; Sadiq et al., 2021; Song et al., 2014; Stanford et al., 2022). Moreover, studies utilizing longitudinal data will be required to better delineate changes that occur in the coupling between tau and atrophy along the AD continuum.

Summary

In summary, we report that significant coupling between tau and atrophy was observed in fewer than 25% of the ROIs considered here for analysis. Yet, the extent of coupling between tau and atrophy in rostral middle frontal and paracentral regions mediated the association between Aβ burden and cognition, highlighting the potential significance of this measure in the clinical presentation of AD dementia.

ACKNOWLEDGMENTS AND DISCLOSURES

We thank William Stanford for valuable feedback. Research reported in this publication was supported by the National Institute on Aging of the National Institutes of Health under Award Number R01AG062590. We would also like to acknowledge NSF DMS-2113662 and NSF RTG grant DMS-2134107 for their support. The content is solely the responsibility of the authors and does not necessarily represent the official views of the National Institutes of Health. Data used in preparation of this article were obtained from the Alzheimer's Disease Neuroimaging Initiative (ADNI) database (adni.loni.usc.edu). As such, the investigators within the ADNI contributed to the design and implementation of ADNI and/or provided data but did not participate in analysis or writing of this report. A complete listing of ADNI investigators can be found at: http://adni.loni.usc.edu/wp-content/uploads/how_to_apply/ADNI_Acknowledgement_List.pdf

Disclosures

The authors have no conflicts of interest or any financial interests to disclose.

References

Biel, D., Luan, Y., Brendel, M., Hager, P., Dewenter, A., Moscoso, A., Otero Svaldi, D., Higgins, I.A., Pontecorvo, M., Römer, S., Steward, A., Rubinski, A., Zheng, L., Schöll, M., Shcherbinin, S., Ewers, M., Franzmeier, N., 2022. Combining tau-PET and fMRI meta-analyses for patient-centered prediction of cognitive decline in Alzheimer's disease. Alzheimers Res Ther 14. https://doi.org/10.1186/s13195-022-01105-5

Boccaletti, S., Bianconi, G., Criado, R., del Genio, C.I., Gómez-Gardeñes, J., Romance, M., Sendiña-Nadal, I., Wang, Z., Zanin, M., 2014. The structure and dynamics of multilayer networks. Phys Rep 544, 1–122. https://doi.org/10.1016/j.physrep.2014.07.001

Cai, L., Wei, X., Liu, J., Zhu, L., Wang, J., Deng, B., Yu, H., Wang, R., 2020. Functional Integration and Segregation in Multiplex Brain Networks for Alzheimer's Disease. Front Neurosci 14. https://doi.org/10.3389/fnins.2020.00051

Chang, Y.L., Jacobson, M.W., Fennema-Notestine, C., Hagler, D.J., Jennings, R.G., Dale, A.M., McEvoy, L.K., 2010. Level of executive function influences verbal memory in amnestic mild cognitive impairment and predicts prefrontal and posterior cingulate thickness. Cerebral Cortex 20. https://doi.org/10.1093/cercor/bhp192

Chang, Y.T., Huang, C.W., Chang, W.N., Lee, J.J., Chang, C.C., 2018. Altered Functional Network Affects Amyloid and Structural Covariance in Alzheimer's Disease. Biomed Res Int 2018. https://doi.org/10.1155/2018/8565620

Contreras, J.A., Avena-Koenigsberger, A., Risacher, S.L., West, J.D., Tallman, E., McDonald, B.C., Farlow, M.R., Apostolova, L.G., Goñi, J., Dzemidzic, M., Wu, Y.C., Kessler, D., Jeub, L., Fortunato, S., Saykin, A.J., Sporns, O., 2019. Resting state network modularity along the prodromal late onset Alzheimer's disease continuum. Neuroimage Clin 22. https://doi.org/10.1016/j.nicl.2019.101687

De Domenico, M., 2017. Multilayer modeling and analysis of human brain networks. Gigascience. https://doi.org/10.1093/gigascience/gix004

De Domenico, M., Porter, M.A., Arenas, A., 2015. MuxViz: A tool for multilayer analysis and visualization of networks. J Complex Netw 3. https://doi.org/10.1093/comnet/cnu038

de Flores, R., Das, S.R., Xie, L., Wisse, L.E.M., Lyu, X., Shah, P., Yushkevich, P.A., Wolk, D.A., 2022. Medial Temporal Lobe Networks in Alzheimer's Disease: Structural and Molecular Vulnerabilities. Journal of Neuroscience 42. https://doi.org/10.1523/JNEUROSCI.0949-21.2021

Desikan, R.S., Ségonne, F., Fischl, B., Quinn, B.T., Dickerson, B.C., Blacker, D., Buckner, R.L., Dale, A.M., Maguire, R.P., Hyman, B.T., Albert, M.S., Killiany, R.J., 2006. An automated labeling system for subdividing the human cerebral cortex on MRI scans into gyral based regions of interest. Neuroimage 31. https://doi.org/10.1016/j.neuroimage.2006.01.021

Digma, L.A., Madsen, J.R., Reas, E.T., Dale, A.M., Brewer, J.B., Banks, S.J., 2019. Tau and atrophy: Domain-specific relationships with cognition. Alzheimers Res Ther 11. https://doi.org/10.1186/s13195-019-0518-8

Guillon, J., Chavez, M., Battiston, F., Attal, Y., La Corte, V., de Schotten, M.T., Dubois, B., Schwartz, D., Colliot, O., Fallani, F.D.V., 2019. Disrupted core-periphery structure of multimodal brain networks in Alzheimer's disease. Network Neuroscience 3. https://doi.org/10.1162/netn_a_00087

Halawa, O.A., Gatchel, J.R., Amariglio, R.E., Rentz, D.M., Sperling, R.A., Johnson, K.A., Marshall, G.A., 2019. Inferior and medial temporal tau and cortical amyloid are associated with daily functional impairment in Alzheimer's disease. Alzheimers Res Ther 11. https://doi.org/10.1186/s13195-019-0471-6

Hammoud, Z., Kramer, F., 2020. Multilayer networks: aspects, implementations, and application in biomedicine. Big Data Anal 5, 1–18. https://doi.org/10.1186/s41044-020-00046-0

Jack, C.R., Bennett, D.A., Blennow, K., Carrillo, M.C., Dunn, B., Haeberlein, S.B., Holtzman, D.M., Jagust, W., Jessen, F., Karlawish, J., Liu, E., Molinuevo, J.L., Montine, T., Phelps, C., Rankin, K.P., Rowe, C.C., Scheltens, P., Siemers, E., Snyder, H.M., Sperling, R., Elliott, C., Masliah, E., Ryan, L., Silverberg, N., 2018. NIA-AA Research Framework: Toward a biological definition of Alzheimer's disease. Alzheimer's & Dementia 14, 535–562. https://doi.org/10.1016/J.JALZ.2018.02.018

Jahanshahi, A.R., Naghdi Sadeh, R., Khezerloo, D., 2023. Atrophy asymmetry in hippocampal subfields in patients with Alzheimer's disease and mild cognitive impairment. Exp Brain Res 241. https://doi.org/10.1007/s00221-022-06543-z

Julkunen, V., Niskanen, E., Muehlboeck, S., Pihlajamäki, M., Könönen, M., Hallikainen, M., Kivipelto, M., Tervo, S., Vanninen, R., Evans, A., Soininen, H., 2009. Cortical thickness analysis to detect progressive mild cognitive impairment: A reference to alzheimer's disease. Dement Geriatr Cogn Disord 28. https://doi.org/10.1159/000256274

Karran, E., Mercken, M., Strooper, B. De, 2011. The amyloid cascade hypothesis for Alzheimer's disease: An appraisal for the development of therapeutics. Nat Rev Drug Discov. https://doi.org/10.1038/nrd3505

Kivelä, M., Arenas, A., Barthelemy, M., Gleeson, J.P., Moreno, Y., Porter, M.A., Kivela, M., Arenas, A., Barthelemy, M., Gleeson, J.P., Moreno, Y., Porter, M.A., 2014. Multilayer networks. J Complex Netw 2, 203–271. https://doi.org/10.1093/comnet/cnu016

Kumar, A., Singh, A., Ekavali, 2015. A review on Alzheimer's disease pathophysiology and its management: An update. Pharmacological Reports. https://doi.org/10.1016/j.pharep.2014.09.004

Kumar, R., Singh, A., 2020. Robustness in Multilayer Networks under Strategical and Random Attacks, in: Procedia Computer Science. https://doi.org/10.1016/j.procs.2020.06.013

Kwak, K., Giovanello, K.S., Bozoki, A., Styner, M., Dayan, E., 2021. Subtyping of mild cognitive impairment using a deep learning model based on brain atrophy patterns. Cell Rep Med 2. https://doi.org/10.1016/j.xcrm.2021.100467

Landau, S.M., Breault, C., Joshi, A.D., Pontecorvo, M., Mathis, C.A., Jagust, W.J., Mintun, M.A., 2013a. Amyloid-β imaging with Pittsburgh compound B and florbetapir: Comparing radiotracers and quantification methods. Journal of Nuclear Medicine 54. https://doi.org/10.2967/jnumed.112.109009

Landau, S.M., Lu, M., Joshi, A.D., Pontecorvo, M., Mintun, M.A., Trojanowski, J.Q., Shaw, L.M., Jagust, W.J., 2013b. Comparing positron emission tomography imaging and cerebrospinal fluid measurements of β-amyloid. Ann Neurol 74. https://doi.org/10.1002/ana.23908

Landau, S.M., Marks, S.M., Mormino, E.C., Rabinovici, G.D., Oh, H., O'Neil, J.P., Wilson, R.S., Jagust, W.J., 2012a. Association of lifetime cognitive engagement and low β-amyloid deposition. Arch Neurol 69. https://doi.org/10.1001/archneurol.2011.2748

Landau, S.M., Mintun, M.A., Joshi, A.D., Koeppe, R.A., Petersen, R.C., Aisen, P.S., Weiner, M.W., Jagust, W.J., 2012b. Amyloid deposition, hypometabolism, and longitudinal cognitive decline. Ann Neurol 72. https://doi.org/10.1002/ana.23650

Langella, S., Mucha, P.J., Giovanello, K.S., Dayan, E., 2021. The association between hippocampal volume and memory in pathological aging is mediated by functional redundancy. Neurobiol Aging 108. https://doi.org/10.1016/j.neurobiolaging.2021.09.002

LaPoint, M.R., Chhatwal, J.P., Sepulcre, J., Johnson, K.A., Sperling, R.A., Schultz, A.P., 2017. The association between tau PET and retrospective cortical thinning in clinically normal elderly. Neuroimage 157. https://doi.org/10.1016/j.neuroimage.2017.05.049

Liu, G., Liu, C., Qiu, A., 2021. Spatial correlation maps of the hippocampus with cerebrospinal fluid biomarkers and cognition in Alzheimer's disease: A longitudinal study. Hum Brain Mapp 42. https://doi.org/10.1002/hbm.25414

Liu, H., Zhang, L., Xi, Q., Zhao, X., Wang, F., Wang, X., Men, W., Lin, Q., 2018. Changes in brain lateralization in patients with mild cognitive impairment and Alzheimer's disease: A resting-state functional magnetic resonance study from Alzheimer's disease neuroimaging initiative. Front Neurol 9. https://doi.org/10.3389/fneur.2018.00003

Liu, X., Maiorino, E., Halu, A., Glass, K., Prasad, R.B., Loscalzo, J., Gao, J., Sharma, A., 2020. Robustness and lethality in multilayer biological molecular networks. Nat Commun 11. https://doi.org/10.1038/s41467-020-19841-3

Liu, Z.Q., Vázquez-Rodríguez, B., Spreng, R.N., Bernhardt, B.C., Betzel, R.F., Misic, B., 2022. Time-resolved structure-function coupling in brain networks. Commun Biol 5. https://doi.org/10.1038/s42003-022-03466-x

Lu, J., Zhang, Z., Wu, P., Liang, X., Zhang, H., Hong, J., Clement, C., Yen, T.C., Ding, S., Wang, M., Xiao, Z., Rominger, A., Shi, K., Guan, Y., Zuo, C., Zhao, Q., 2023. The heterogeneity of asymmetric tau distribution is associated with an early age at onset and poor prognosis in Alzheimer's disease. Neuroimage Clin 38. https://doi.org/10.1016/j.nicl.2023.103416

Maass, A., Landau, S., Horng, A., Lockhart, S.N., Rabinovici, G.D., Jagust, W.J., Baker, S.L., La Joie, R., 2017. Comparison of multiple tau-PET measures as biomarkers in aging and Alzheimer's disease. Neuroimage 157, 448–463. https://doi.org/10.1016/j.neuroimage.2017.05.058

Mak, E., Bethlehem, R.A.I., Romero-Garcia, R., Cervenka, S., Rittman, T., Gabel, S., Surendranathan, A., Bevan-Jones, R.W., Passamonti, L., Vázquez Rodríguez, P., Su, L., Arnold, R., Williams, G.B., Hong, Y.T., Fryer, T.D., Aigbirhio, F.I., Rowe, J.B., O'Brien, J.T., 2018. In vivo coupling of tau pathology and cortical thinning in Alzheimer's disease. Alzheimer's and Dementia: Diagnosis, Assessment and Disease Monitoring 10. https://doi.org/10.1016/j.dadm.2018.08.005

Minkova, L., Habich, A., Peter, J., Kaller, C.P., Eickhoff, S.B., Klöppel, S., 2017. Gray matter asymmetries in aging and neurodegeneration: A review and meta-analysis. Hum Brain Mapp 38. https://doi.org/10.1002/hbm.23772

Mohanty, R., Ferreira, D., Nordberg, A., Westman, E., 2023. Associations between different tau-PET patterns and longitudinal atrophy in the Alzheimer's disease continuum: biological and methodological perspectives from disease heterogeneity. Alzheimers Res Ther 15. https://doi.org/10.1186/s13195-023-01173-1

Nichols, E., Szoeke, C.E.I., Vollset, S.E., Abbasi, N., Abd-Allah, F., Abdela, J., Aichour, M.T.E., Akinyemi, R.O., Alahdab, F., Asgedom, S.W., Awasthi, A., Barker-Collo, S.L., Baune, B.T., Béjot, Y., Belachew, A.B., Bennett, D.A., Biadgo, B., Bijani, A., Bin Sayeed, M.S., Brayne, C., Carpenter, D.O., Carvalho, F., Catalá-López, F., Cerin, E., Choi, J.Y.J., Dang, A.K., Degefa, M.G., Djalalinia, S., Dubey, M., Duken, E.E., Edvardsson, D., Endres, M., Eskandarieh, S., Faro, A., Farzadfar, F., Fereshtehnejad, S.M., Fernandes, E., Filip, I., Fischer, F., Gebre, A.K., Geremew, D., Ghasemi-Kasman, M., Gnedovskaya, E. V., Gupta, R., Hachinski, V., Hagos, T.B., Hamidi, S., Hankey, G.J., Haro, J.M., Hay, S.I., Irvani, S.S.N., Jha, R.P., Jonas, J.B., Kalani, R., Karch, A., Kasaeian, A., Khader, Y.S., Khalil, I.A., Khan, E.A., Khanna, T., Khoja, T.A.M., Khubchandani, J., Kisa, A., Kissimova-Skarbek, K., Kivimäki, M., Koyanagi, A., Krohn, K.J., Logroscino, G., Lorkowski, S., Majdan, M., Malekzadeh, R., März, W., Massano, J., Mengistu, G., Meretoja, A., Mohammadi, M., Mohammadi-Khanaposhtani, M., Mokdad, A.H., Mondello, S., Moradi, G., Nagel, G., Naghavi, M., Naik, G., Nguyen, L.H., Nguyen, T.H., Nirayo, Y.L., Nixon, M.R., Ofori-Asenso, R., Ogbo, F.A., Olagunju, A.T., Owolabi, M.O., Panda-Jonas, S., Passos, V.M. de A., Pereira, D.M., Pinilla-Monsalve, G.D., Piradov, M.A., Pond, C.D., Poustchi, H., Qorbani, M., Radfar, A., Reiner, R.C., Robinson, S.R., Roshandel, G., Rostami, A., Russ, T.C., Sachdev, P.S., Safari, H., Safiri, S., Sahathevan, R., Salimi, Y., Satpathy, M., Sawhney, M., Saylan, M., Sepanlou, S.G., Shafieesabet, A., Shaikh, M.A., Sahraian, M.A., Shigematsu, M., Shiri, R., Shiue, I., Silva, J.P., Smith, M., Sobhani, S., Stein, D.J., Tabarés-Seisdedos, R., Tovani-Palone, M.R., Tran, B.X., Tran, T.T., Tsegay, A.T., Ullah, I., Venketasubramanian, N., Vlassov, V., Wang, Y.P., Weiss, J., Westerman, R., Wijeratne, T., Wyper, G.M.A., Yano, Y., Yimer, E.M., Yonemoto, N., Yousefifard, M., Zaidi, Z., Zare, Z., Vos, T., Feigin, V.L., Murray, C.J.L., 2019. Global, regional, and national burden of Alzheimer's disease and other dementias, 1990–2016: a systematic analysis for the Global Burden of Disease Study 2016. Lancet Neurol 18. https://doi.org/10.1016/S1474-4422(18)30403-4

O'Bryant, S.E., 2008. Staging Dementia Using Clinical Dementia Rating Scale Sum of Boxes Scores. Arch Neurol 65. https://doi.org/10.1001/archneur.65.8.1091

Ossenkoppele, R., Iaccarino, L., Schonhaut, D.R., Brown, J.A., La Joie, R., O'Neil, J.P., Janabi, M., Baker, S.L., Kramer, J.H., Gorno-Tempini, M.L., Miller, B.L., Rosen, H.J., Seeley, W.W., Jagust, W.J., Rabinovici, G.D., 2019. Tau covariance patterns in Alzheimer's disease patients match intrinsic connectivity networks in the healthy brain. Neuroimage Clin 23. https://doi.org/10.1016/j.nicl.2019.101848

Pereira, J.B., Harrison, T.M., La Joie, R., Baker, S.L., Jagust, W.J., 2020. Spatial patterns of tau deposition are associated with amyloid, ApoE, sex, and cognitive decline in older adults. Eur J Nucl Med Mol Imaging 47. https://doi.org/10.1007/s00259-019-04669-x

Radicchi, F., Bianconi, G., 2017. Redundant interdependencies boost the robustness of multiplex networks. Phys Rev X 7. https://doi.org/10.1103/PhysRevX.7.011013

Ricciarelli, R., Fedele, E., 2017. The Amyloid Cascade Hypothesis in Alzheimer's Disease: It's Time to Change Our Mind. Curr Neuropharmacol 15. https://doi.org/10.2174/1570159x15666170116143743

Robitaille, A.L., Webber, Q.M.R., Turner, J.W., Vander Wal, E., 2021. The problem and promise of scale in multilayer animal social networks. Curr Zool 67. https://doi.org/10.1093/cz/zoaa052

Sadiq, M.U., Langella, S., Giovanello, K.S., Mucha, P.J., Dayan, E., 2021. Accrual of functional redundancy along the lifespan and its effects on cognition. Neuroimage 229. https://doi.org/10.1016/j.neuroimage.2021.117737

Sepulcre, J., Schultz, A.P., Sabuncu, M., Gomez-Isla, T., Chhatwal, J., Becker, A., Sperling, R., Johnson, K.A., 2016. In vivo tau, amyloid, and gray matter profiles in the aging brain. Journal of Neuroscience 36. https://doi.org/10.1523/JNEUROSCI.0639-16.2016

Shimada, Y., Hirata, Y., Ikeguchi, T., Aihara, K., 2016. Graph distance for complex networks. Sci Rep 6. https://doi.org/10.1038/srep34944

Song, J., Birn, R.M., Boly, M., Meier, T.B., Nair, V.A., Meyerand, M.E., Prabhakaran, V., 2014. Age-related reorganizational changes in modularity and functional connectivity of human brain networks. Brain Connect 4. https://doi.org/10.1089/brain.2014.0286

Stanford, W.C., Mucha, P.J., Dayan, E., 2022. A robust core architecture of functional brain networks supports topological resilience and cognitive performance in middle-and old-aged adults. https://doi.org/10.1073/pnas

Taylor, D., Caceres, R.S., Mucha, P.J., 2017. Super-resolution community detection for layer-aggregated multilayer networks. Phys Rev X 7, 1–12. https://doi.org/10.1103/PhysRevX.7.031056

Team, R.C., 2021. R: A Language and Environment for Statistical Computing. R Foundation for Statistical Computing.

Timmers, T., Ossenkoppele, R., Wolters, E.E., Verfaillie, S.C.J., Visser, D., Golla, S.S.V., Barkhof, F., Scheltens, P., Boellaard, R., Van Der Flier, W.M., Van Berckel, B.N.M., 2019. Associations between quantitative [18F]flortaucipir tau PET and atrophy across the Alzheimer's disease spectrum. Alzheimers Res Ther 11. https://doi.org/10.1186/s13195-019-0510-3

Wilson, J.D., Palowitch, J., Bhamidi, S., Nobel, A.B., 2017. Community extraction in multilayer networks with heterogeneous community structure. Journal of Machine Learning Research 18.

Xia, C., Makaretz, S.J., Caso, C., McGinnis, S., Gomperts, S.N., Sepulcre, J., Gomez-Isla, T., Hyman, B.T., Schultz, A., Vasdev, N., Johnson, K.A., Dickerson, B.C., 2017. Association of in vivo [18F]AV-1451 tau PET imaging results with cortical atrophy and symptoms in typical and atypical Alzheimer disease. JAMA Neurol 74. https://doi.org/10.1001/jamaneurol.2016.5755

Yang, H., Xu, H., Li, Q., Jin, Y., Jiang, W., Wang, J., Wu, Y., Li, W., Yang, C., Li, X., Xiao, S., Shi, F., Wang, T., 2019. Study of brain morphology change in Alzheimer's disease and amnestic mild cognitive impairment compared with normal controls. Gen Psychiatr 32. https://doi.org/10.1136/gpsych-2018-100005

Young, C.B., Landau, S.M., Harrison, T.M., Poston, K.L., Mormino, E.C., 2021. Influence of common reference regions on regional tau patterns in cross-sectional and longitudinal [18F]-AV-1451 PET data. Neuroimage 243. https://doi.org/10.1016/j.neuroimage.2021.118553

Yun, J.Y., Boedhoe, P.S.W., Vriend, C., Jahanshad, N., Abe, Y., Ameis, S.H., Anticevic, A., Arnold, P.D., Batistuzzo, M.C., Benedetti, F., Beucke, J.C., Bollettini, I., Bose, A., Brem, S., Calvo, A., Cheng, Y., Cho, K.I.K., Ciullo, V., Dallaspezia, S., Denys, D., Feusner, J.D., Fouche, J.P., Giménez, M., Gruner, P., Hibar, D.P., Hoexter, M.Q., Hu, H., Huyser, C., Ikari, K., Kathmann, N., Kaufmann, C., Koch, K., Lazaro, L., Lochner, C., Marques, P., Marsh, R., Martínez-Zalacaín, I., Mataix-Cols, D., Menchón, J.M., Minuzzi, L., Morgado, P., Moreira, P., Nakamae, T., Nakao, T., Narayanaswamy, J.C., Nurmi, E.L., O'Neill, J., Piacentini, J., Piras, Fabrizio, Piras, Federica, Janardhan Reddy, Y.C., Sato, J.R., Blair Simpson, H., Soreni, N., Soriano-Mas, C., Spalletta, G., Stevens, M.C., Szeszko, P.R., Tolin, D.F., Venkatasubramanian, G., Walitza, S., Wang, Z., Van Wingen, G.A., Xu, J., Xu, X., Zhao, Q., Thompson, P.M., Stein, D.J., Van Den Heuvel, O.A., Kwon, J.S., 2020. Brain structural covariance networks in obsessive-compulsive disorder: A graph analysis from the ENIGMA consortium. Brain 143, 684–700. https://doi.org/10.1093/brain/awaa001

Yun, J.Y., Jang, J.H., Kim, S.N., Jung, W.H., Kwon, J.S., 2015. Neural Correlates of Response to Pharmacotherapy in Obsessive-Compulsive Disorder: Individualized Cortical Morphology-Based Structural Covariance. Prog Neuropsychopharmacol Biol Psychiatry 63. https://doi.org/10.1016/j.pnpbp.2015.06.009

Figure Legends

Figure 1: Modeling framework. (A.) Participants' (MCI, CN) tau standardized uptake value ratios (SUVRs) were calculated in 70 regions of interest (ROIs) (B.) Volumetric measures from the same ROIs were used as measures of atrophy. Data was Z-score transformed using means and standard-deviations (SD) from controls (Value – Mean [CN]/ SD[CN]) (C.) Individual-subject structural covariance matrices were reconstructed for tau and atrophy (D.) Covariance matrices for tau and atrophy were then modeled as single layer networks for each individual participant. (E.) Multilayer networks with tau and atrophy serving as single layers were reconstructed and labeled according to A□ positivity. (F.) Inter-layer (yellow), Intra-layer (green) and cross-layer (grey-dotted) edges in a multilayer network. MCI – Mild Cognitive Impairment, CN – cognitively normal controls.

Figure 2: Coupling between tau and atrophy. (A.) The A□+ group showed greater tau uptake than the A□- group averaged across all ROIs. (B.) The A□+ group also showed higher atrophy levels when compared to the A□- group across all ROIs. (C.) Calculation of coupling scores computed to measure the relative coupling between tau and atrophy, was based on the Euclidean distance between layers (distance matrix D) and denotes the ratio between a spatially coupled edge D_r (red) and all other non-coupled edges D_b (black). (D.) ROIs that showed significantly higher coupling in the A□+ group, as compared to the A□- group (FDR corrected).

Figure 3: Mediational link between A□ burden, coupling between tau and atrophy and global cognition. The association between A□ burden, considered as a continuous variable, and global cognition (CDR-SB: Clinical Dementia Rating Scale–Sum of Boxes) was mediated by coupling between tau and atrophy in the right rostral middle frontal ($p<0.05$) and right paracentral ($p<0.05$) cortices. Direct, indirect (mediation) and direct effects are shown.

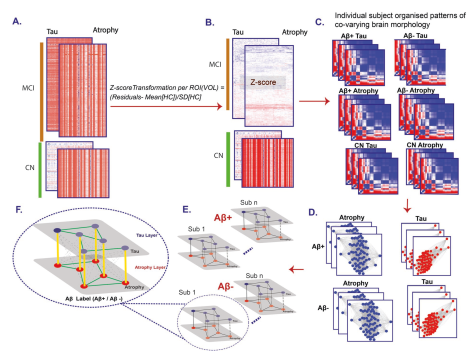
A.
Tau
Atrophy
MCI
CN
Z-scoreTransformation per ROI(VOL) =
(Residuals- Mean[HC])/SD[HC]
B.
Tau
Atrophy
MCI
Z-score
CN
C.
Individual subject organised patterns of
co-varying brain morphology
Aβ+ Tau
Aβ- Tau
Aβ+ Atrophy
Aβ- Atrophy
CN Tau
CN Atrophy
D.
Atrophy
Tau
Aβ+
Atrophy
Tau
Aβ-
E.
Aβ+
Sub 1
Sub n
Aβ-
Sub 1
Sub n
F.
Tau Layer
Atrophy Layer
Aβ Label (Aβ+ / Aβ -)

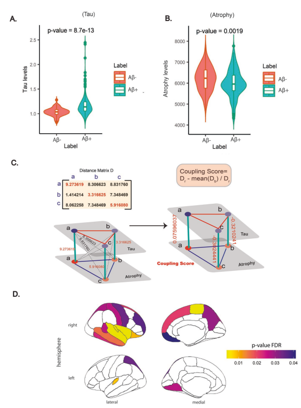
A.
(Tau)
p-value = 8.7e-13
Tau levels
2.5
2.0
1.5
1.0
Aβ-
Aβ+
Label
Label
Aβ-
Aβ+
B.
(Atrophy)
p-value = 0.0019
Atrophy levels
8000
7000
6000
5000
4000
Aβ-
Aβ+
Label
Label
Aβ-
Aβ+
C.
Distance Matrix D
a b c
a 9.273619 8.306623 8.831760
b 1.414214 3.316625 7.348469
c 8.062258 7.348469 5.916080
Coupling Score=
D_r - mean(D_b) / D_r
Tau
Atrophy
9.273619
3.316625
5.916080
0.07596037
-0.3210241
-0.3024441
Coupling Score
D.
right
left
hemisphere
lateral
medial
side
p-value FDR
0.01
0.02
0.03
0.04

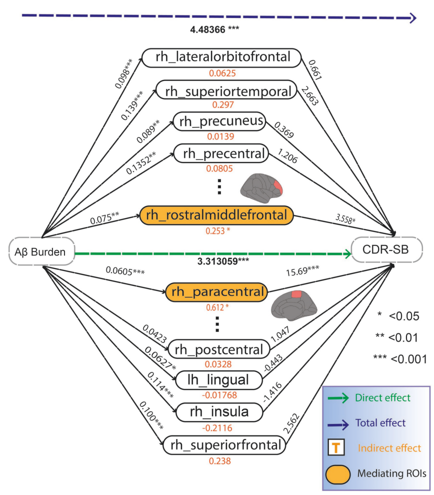

4.48366 ***
rh_lateralorbitofrontal
0.098***
0.661
0.0625
rh_superiortemporal
0.139***
2.663
0.297
rh_precuneus
0.089**
0.369
0.0139
rh_precentral
0.1352**
1.206
0.0805
rh_rostralmiddlefrontal
0.075**
3.558*
0.253 *
Aβ Burden
CDR-SB
3.313059***
rh_paracentral
0.0605***
15.69***
0.612 *
rh_postcentral
0.0423
1.047
0.0328
lh_lingual
0.0627*
-0.443
-0.01768
rh_insula
0.114***
-1.416
-0.2116
rh_superiorfrontal
0.100***
2.562
0.238
* <0.05
** <0.01
*** <0.001
Direct effect
Total effect
T
Indirect effect
Mediating ROIs